Original Article

# Cardiac Hypertrophy is Positively Regulated by MicroRNA-24 in Rats

**Juan Gao, Min Zhu, Rui-Feng Liu, Jian-Shu Zhang, Ming Xu**

Department of Cardiology and Institute of Vascular Medicine, Peking University Third Hospital; Key Laboratory of Cardiovascular Molecular Biology and Regulatory Peptides, Ministry of Health; Key Laboratory of Molecular Cardiovascular Science, Ministry of Education; Beijing Key Laboratory of Cardiovascular Receptors Research, Beijing 100191, China

## Abstract

**Background:** MicroRNA-24 (miR-24) plays an important role in heart failure by reducing the efficiency of myocardial excitation-contraction coupling. Prolonged cardiac hypertrophy may lead to heart failure, but little is known about the role of miR-24 in cardiac hypertrophy. This study aimed to preliminarily investigate the function of miR-24 and its mechanisms in cardiac hypertrophy.

**Methods:** Twelve Sprague-Dawley rats with a body weight of 50 ± 5 g were recruited and randomly divided into two groups: a transverse aortic constriction (TAC) group and a sham surgery group. Hypertrophy index was measured and calculated by echocardiography and hematoxylin and eosin staining. TargetScans algorithm-based prediction was used to search for the targets of miR-24, which was subsequently confirmed by a real-time polymerase chain reaction and luciferase assay. Immunofluorescence labeling was used to measure the cell surface area, and $^{3}$H-leucine incorporation was used to detect the synthesis of total protein in neonatal rat cardiac myocytes (NRCMs) with the overexpression of miR-24. In addition, flow cytometry was performed to observe the alteration in the cell cycle. Statistical analysis was carried out with GraphPad Prism v5.0 and SPSS 19.0. A two-sided $P < 0.05$ was considered as the threshold for significance.

**Results:** The expression of miR-24 was abnormally increased in TAC rat cardiac tissue ($t = -2.938$, $P < 0.05$). TargetScans algorithm-based prediction demonstrated that CDKN1B (p27, Kip1), a cell cycle regulator, was a putative target of miR-24, and was confirmed by luciferase assay. The expression of p27 was decreased in TAC rat cardiac tissue ($t = 2.896$, $P < 0.05$). The overexpression of miR-24 in NRCMs led to the decreased expression of p27 ($t = 4.400$, $P < 0.01$), and decreased G0/G1 arrest in cell cycle and cardiomyocyte hypertrophy.

**Conclusion:** MiR-24 promotes cardiac hypertrophy partly by affecting the cell cycle through down-regulation of p27 expression.

**Key words:** Cardiac Hypertrophy; Cell Cycle; MicroRNA; MicroRNA-24; p27

## Introduction

Cardiac hypertrophy has long been known as an independent risk factor for cardiac morbidity and all-cause mortality.[1,2] It is an adaptive mechanism which is beneficial in the short term. However, prolonged cardiac hypertrophy ultimately leads to heart failure and death. Even with normal cardiac function in the early stage of cardiac hypertrophy, the cardiomyocytes undergo phenotypic changes such as increased cell size.[3] Although considerable efforts have been made to unravel the molecular mechanism underlying the changes that occur during cardiac hypertrophy and heart failure, the molecular mechanisms remain elusive.[3-5] MicroRNAs (miRNAs) are small conserved RNA molecules of about 22 nucleotides which modulate gene expression in human and animals, primarily through base pairing to the 3' untranslated region (3'UTR) of target mRNAs and lead to mRNA cleavage and/or translation repression.[6] Increasing evidence has indicated that miRNAs play a key role in cardiac hypertrophy.[7-10]

Our previous studies showed that microRNA-24 (miR-24 expression level was significantly increased in the cardiac tissue of heart failure from both rats and human.[11] In heart failure animal models, abnormally higher expression of miR-24

Access this article online

Quick Response Code:

Website: www.cmj.org

DOI: 10.4103/0366-6999.232793

**Address for correspondence:** Dr. Ming Xu, Department of Cardiology and Institute of Vascular Medicine, Peking University Third Hospital; Key Laboratory of Cardiovascular Molecular Biology and Regulatory Peptides, Ministry of Health; Key Laboratory of Molecular Cardiovascular Science, Ministry of Education; Beijing Key Laboratory of Cardiovascular Receptors Research, Beijing 100191, China
E-Mail: xuminghi@bjmu.edu.cn



**Received:** 23-01-2018 **Edited by:** Yuan-Yuan Ji

**How to cite this article:** Gao J, Zhu M, Liu RF, Zhang JS, Xu M. Cardiac Hypertrophy is Positively Regulated by MicroRNA-24 in Rats. Chin Med J 2018;131:1333-41.

led to decreased efficiency of excitation-contraction coupling by down-regulating its target gene of Junctophilin-2.[12] Since target genes of miR-24 are different, we performed a miRNA functional enrichment analysis using TAM (tool for annotation of microRNA, a method for enrichment and depletion analysis of a miRNA category in a list of miRNAs).[13] The results showed that miR-24 was closely related with muscle development which is an important pathological basis of heart failure. In addition, the biological analysis showed that miR-24 was associated with cell cycle in cancer cells and cell proliferation. In cardiomyocytes, the activity of cell cycle controls cell proliferation, which plays an important role in cardiac hypertrophy.[14] These findings intrigued us to investigate the role of miR-24 in cardiac hypertrophy and its potential targets.

In the present study, we aimed to investigate the function of miR-24 in cardiac hypertrophy by establishing a transverse aortic constriction (TAC) rat model, and miR-24 overexpressing in neonatal rat cardiac myocytes (NRCMs). The underlying mechanisms of miR-24 in cardiac hypertrophy were also investigated by TargetScans algorithm-based prediction, luciferase assay, and flow cytometry.

## Methods

### Ethical approval

All the animal experiments were carried out according to the Guide for Care, and the use of Laboratory Animals published by the US National Institutes of Health (NIH Publication No. 85e23, revised 2011), and the study protocol was approved by the Institutional Animal Care and Use Committee of Peking University (No. LA2016145). Every effort was made to reduce the number of animals and minimize their suffering.

### Transverse aortic constriction rat model

A 4-week-old wild-type male Sprague-Dawley (SD) rats weighing 50 ± 5 g were obtained from the Medical Experimental Animal Center of Peking University, Beijing, China. The rats were divided into two groups: sham group ($n$ = 6) and TAC group ($n$ = 6). TAC and sham were induced as described previously.[15] Briefly, rats were anesthetized by intraperitoneal (i.p.) administration of 50 mg/kg pentobarbital (Merck, Whitehouse Station, NJ, USA). A longitudinal cut was made in the proximal portion of the sternum. The aorta under the upper left sternal border was ligated with a 27-gauge needle using 7-0 silk surgical thread. After ligation, the needle was promptly removed, and the thoracic cavity was closed. The sham procedure was identical except that the aorta was not ligated.

### Echocardiography

Vevo2100 system (VisualSonics Inc., Toronto, Ontario, Canada) was used to evaluate cardiac structure and systolic function of rats. In brief, rats were anesthetized with 2.0% isoflurane (Baxter Healthcare Corp., CA, USA) until the heart rate was stabilized at about 400 beats/min. Parasternal long-axis images were acquired in B-mode with the maximum left ventricle length identified. The M-mode cursor was positioned perpendicularly to the maximum left ventricle dimension in end-diastole and systole, and M-mode images were obtained for measuring wall thickness and chamber dimensions.

### Neonatal rat cardiac myocytes culture

Cardiomyocytes isolated and cultured from newborn SD rats aged 1–2 days were obtained from the Medical Experimental Animal Center of Peking University. NRCMs were prepared as previously described.[16] In brief, central thoracotomy was performed in neonatal rats under anesthesia with 1.0% isoflurane. Hearts were quickly excised and immediately embedded in freezing Hank's Balanced Salt Solution (Thermo Fisher Scientific, MA, USA). Cardiomyocytes were dispersed by digestion with 0.25% trypsin (Gibco, NY, USA) and 0.05% collagenase II (Sigma, MO, USA) at 37°C. The isolated cardiomyocytes were then cultured with 10% fetal bovine serum (Hyclone, UT, USA) and antibiotics (50 U/ml penicillin and 50 mg/ml streptomycin) at 37°C in 5% $CO_2$.

### Quantitative reverse transcriptase-polymerase chain reaction analysis

Total RNA, containing miRNA, was extracted from cardiac tissues and NRCMs using miRNeasy Kits (QIAGEN, Germany), and genomic DNA was removed using a DNA-free kit (Invitrogen, CA, USA) following the manufacturer's instructions. First-strand cDNA was synthesized by miRNA-specific reverse-transcription primers (RiboBio Co., Ltd, China) (for miR-24) or oligodT15 (for p27) using SuperScript III Reverse Transcriptase (Invitrogen). One microgram of cDNA was included for real-time polymerase chain reaction (RT-PCR) amplification using the Brilliant II SYBR Green qPCR Master Mix (Stratagene, CA, USA), and the fluorescent signals were monitored with n Mx3000p Real-Time PCR System (Stratagene). The small nuclear RNA, U6, was used as control for miRNA samples, and glyceraldehyde 3-phosphate dehydrogenase was used as control for p27 mRNA quantification.

### Measurement of cell surface area by immunofluorescence

NRCMs were seeded in 12-well plates at a concentration of $5 \times 10^5$ cells/ml. Over-expression of miR-24 was achieved following adenovirus transfection. After treatment for 24 h, the cells were fixed with 4% paraformaldehyde at 37°C for 15 min. After washing with phosphate-buffered saline (PBS), the cells were permeabilized with 2% Triton X-100 in PBS at 37°C for 30 min. After washing with PBS, the nuclei were stained with phalloidin (1:50–1:100; Sigma) at 37°C for 60 min. Immunofluorescence was determined using a fluorescence microscope (Leica, Germany). An average of 150 cardiomyocytes from 30 fields was chosen at random for measurement of cell size. Immunofluorescence images captured from cardiomyocytes stained with Texas red phalloidin were measured using the ImageJ Particle Analyzer algorithm.

### Protein extracts and Western blotting

Proteins from heart tissue and NRCMs were extracted in buffer containing 1% sodium deoxycholate, 10 mmol/L

$Na_4P_2O_7$, 1% Triton X-100, 10% glycerol, 150 mmol/L NaCl, 5 mmol/L EDTA-$Na_2$, 50 mmol/L Tris (pH 7.4), 0.1% SDS, 50 mmol/L NaF, 1 mmol/L $Na_3VO_4$, 1 mmol/L PMSF, and protease inhibitor cocktail (Roche, Switzerland). The proteins which were separated by SDS-PAGE were transferred to nitrocellulose membranes. The membranes were incubated with primary antibodies and then probed with horseradish peroxidase-conjugated secondary antibodies. Blots were visualized using an enhanced chemiluminescence kit (Amersham Biosciences Inc., CT, USA). Primary antibodies used for Western blotting in this study were p27 (Abcam, UK, dilution 1:500) and EIF5 (Cell Signaling Technology, MA, USA, dilution 1:5000).

### Plasmid construction and luciferase assay

Human embryonic kidney HEK-293A cells were seeded at a concentration of 50,000 cells/well in 24-well plates. One construct contained the wild-type p27 3'UTR region with the miR-24 binding site intact (p27-WT). A matched control construct contained mutated bases in the miR-24 binding site (AAAGGUUGCAUA-cugagccA changed to AAAGGUUGCAUA-agtctaaA) (p27-MUT) (Shanghai Genechem Co., Ltd. China). HEK-293A cells were transfected with 500 ng of either p27-WT plasmid or p27-MUT, together with either mimic miR-24 (RiboBio Co., Ltd) or nontargeting negative control (scramble) at a concentration of 50 nM. Lipofectamine 2000 reagent (Invitrogen) was used for the transfection, and 50 ng Renilla luciferase vector was included in each well to control the transfection efficiency. Twenty-four hours after transfection, luciferase activity was measured using a Dual-Luciferase Reporter Assay System (Promega Corporation, WI, USA); and the firefly luciferase activity was normalized to Renilla luciferase activity.

### Flow cytometry

NRCMs were harvested at the indicated time points, washed, fixed, and centrifuged (1500 ×*g*), and then labeled with propidium iodide (Invitrogen). Flow cytometric analysis was carried out on a FACScan Q4 (Becton Dickinson, CA, USA) cell sorter. Percentages of cells in G0-G1, S, and G2-M phases were calculated with Mod Fit software (Verity Software House, USA) for Windows.

### Measurement of total protein content by $^3$H leucine incorporation assay

NRCMs were seeded in 24-well plates at a concentration of $1 \times 10^5$ cells/ml. $^3$H-leu (1 uci/ml) was added for 12 h before the cells were harvested. After washing with PBS, the cells were treated with precooled 10% trichloroacetic acid for 30 min on ice. The cell lysate was added and incubated at 37°C overnight so that the cells were fully cracked. Each sample was transferred to the flicker bottle according to the proportion of 0.5 ml cell lysate in the 6 ml scintillation liquid. The lid was covered, and the samples were shaken and mixed well, and counts per minute (CPM) and disintegrations per minute value were read on the stroboscope (Hidex 300SL, Finland).

### Hematoxylin and eosin and Sirius Red staining

The left ventricular ischemic tissue from the rats was fixated by 4% for 24 h, then paraffin-embedded and sectioned at a 4-μm thickness through a rotary microtome. Hematoxylin and eosin (H and E) and Sirius Red staining was used to detect morphologic changes of cardiac myocytes and the degree of myocardial fibrosis as previously described.[17]

### Statistical analysis

Statistical analysis was carried out with GraphPad Prism v5.0 (GraphPad Software Inc., San Diego, California, USA) and SPSS 19.0 (IBM Corp, Armonk, NY, USA). The Shapiro-Wilk was used to test the normal distribution in the continuous data, and the Levene's test was used to detect the equality of variances. Consistent with the measurement data, normal distribution was expressed as mean ± standard error (SE), and the independent samples Student's *t*-test was used to detect the differences between groups. If the data distribution was not normal, the Mann-Whitney test was employed for the nonparametric analysis. In all analyses, a two-sided $P < 0.05$ was considered as the threshold for significance.

## Results

### Expression of microRNA-24 was increased in the left ventricular tissue of transverse aortic constriction rats

TAC was an established *in vivo* model of hemodynamic overload,[18] which induced significant and equivalent left ventricle pressure load in SD rats. Expression of the hypertrophic marker genes, atrial natriuretic factor (ANP) and brain natriuretic peptide (BNP) was increased following TAC injury (ANP: 0.93 ± 0.15 vs. 0.50 ± 0.07, $P < 0.05$; BNP: 0.04 ± 0.01 vs. 0.02 ± 0.00, $t = -3.676$, $P < 0.01$) [Figure 1a and 1b]. TAC rats exhibited cardiac hypertrophic pathological changes by H and E staining compared with the sham group, and the myocardial cross-sectional area in the TAC group was significantly increased compared with the sham group (6307 ± 681 μm$^2$ vs. 3470 ± 260 μm$^2$, $t = -3.890$, $P < 0.01$) [Figure 1c]. The Sirius Red staining of the heart showed that the fibrosis area in TAC rats was also increased compared with the sham group (62.50% ± 0.01% vs. 13.10% ± 0.03%, $t = -3.344$, $P < 0.01$) [Supplementary Figure 1]. Echocardiography revealed that the left ventricular posterior wall thickness at diastole and left ventricular mass were both increased following TAC injury (2.61 ± 0.17 mm vs. 1.91 ± 0.10 mm, $t = -3.564$, $P < 0.01$; 1469.0 ± 140.6 mg vs. 969.1 ± 34.2 mg, $t = -3.453$, $P < 0.01$) [Figure 1d]. In addition, the heart weight-to-body weight ratio and the heart weight-to-tibia length ratio were also elevated following TAC injury [Supplementary Table 1]. Quantitative RT-PCR (qRT-PCR) analysis was conducted to determine the expression of miR-24 in heart tissue of the TAC rat model. As shown in Figure 1e, increased expression level of miR-24 was observed in rat hypertrophic hearts induced by 6 weeks of TAC injury (2.61 ± 0.17 vs. 1.91 ± 0.10, $t = -2.938$, $P < 0.05$), suggesting that miR-24 was involved in cardiac hypertrophy.

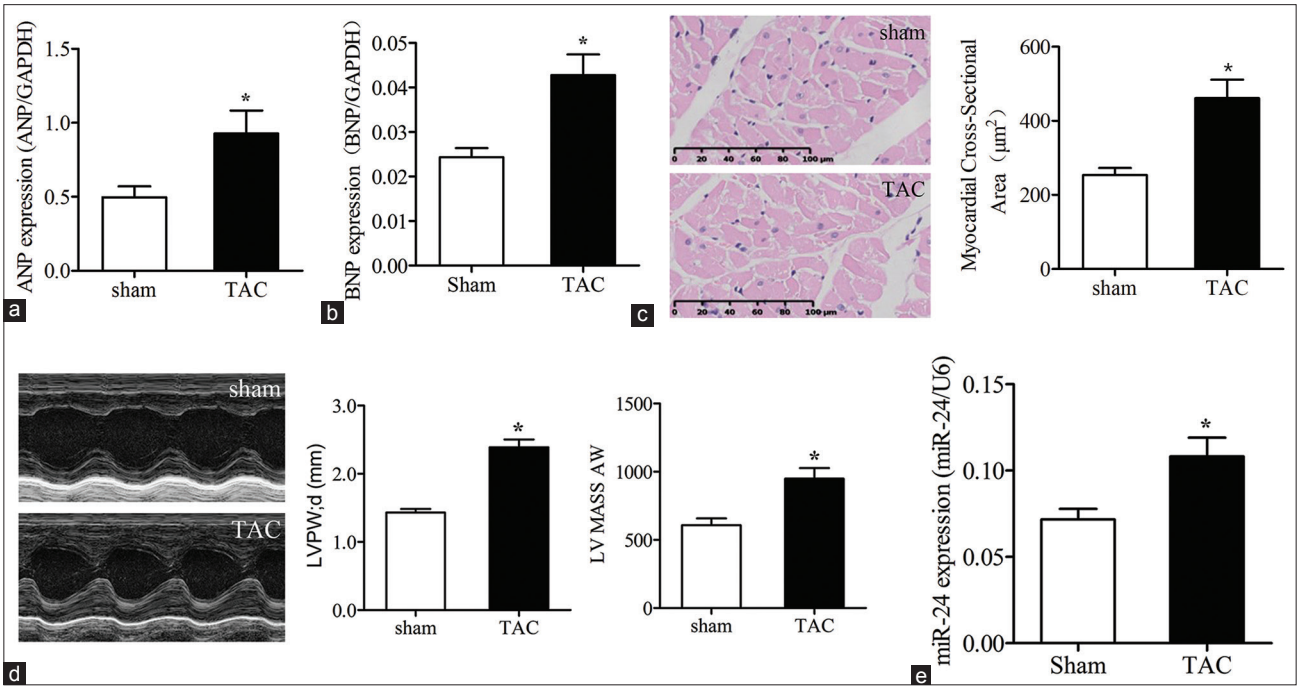


**Figure 1:** Expression of miR-24 increased in rat hypertrophic cardiac tissues. (a) The expression of ANP increased in TAC rats. *$P < 0.05$ versus sham. (b) The expression of BNP increased in TAC rats. *$P < 0.05$ versus sham. (c) The myocardial cross-sectional area increased in TAC rats (H&E staining, original magnification ×30). *$P < 0.05$ versus sham. (d) Echocardiography revealed the increase of LVPW; d and LV mass AW in TAC rats. *$P < 0.05$ versus sham. (e) The expression of miR-24 increased in TAC rats. *$P < 0.05$ versus sham. Data are shown as mean ± SE, $n = 6$. ANP: Atrial natriuretic factor; TAC: Transverse aortic constriction; BNP: Brain natriuretic peptide; LVPW;d: Left ventricular posterior diastolic wall thickness; SE: Standard error; LV mass AW: Left ventricular mass AW.

## Expression of p27 was repressed by microRNA-24 in hypertrophic cardiac tissue and Neonatal rat cardiac myocytes

To determine the mechanism by which miR-24 regulates cardiac hypertrophy, we used the TargetScans algorithm (http://www.TargetScans.org) to search for the targets of miR-24. As shown in Table 1, priorities were given to both human and rat targets, to higher expression in heart tissue, and to targets with clearly studied functions. The aggregate $P_{CT}$ value (the probability of conserved targeting) derived from the TargetScans software was also considered [Supplementary Figure 2]. Six potential targets of miR-24 were included in this study. qRT-PCR was performed to detect the expression of the screened targets following overexpression of miR-24 in NRCMs. The results showed that the expression of CDKN1B (p27, Kip1) was significantly decreased (0.69 ± 0.07 vs. 1.00 ± 0.03, $t = 3.108$, $P < 0.01$) [Figure 2a]. Interestingly, in contrast to increased expression of miR-24 in hypertrophic cardiac tissue, the expression of p27 mRNA exhibited a 40.35% reduction (0.01 ± 0.00 vs. 0.02 ± 0.00, $t = 2.896$, $P < 0.05$) [Figure 2b]. The protein level of p27 exhibited a 40.80% reduction in hypertrophic cardiac tissue (5.95 ± 0.44 vs. 10.05 ± 0.83, $P < 0.01$) [Figure 2c].

To further confirm the regulation mechanism of miR-24 in p27 expression, we performed luciferase reporter assays in HEK-293A cells. As indicated in Figure 2d, co-transfection of miR-24 mimics with wild-type pMIR-p27-3'UTR resulted in a significant decrease in luciferase activity (miR-24-p27 WT vs. scramble-p27: 0.30 ± 0.02 vs. 0.99 ± 0.01, $t = 30.552$, $P < 0.001$). However, there was no decreased luciferase activity by co-transfection of miR-24 mimics with constructs containing mutated pMIR-p27-3'UTR sequences [Figure 2d]. In addition, miR-24 overexpression adenoviral expression vectors (AEVs) and negative control with only inserted Green Fluorescent Protein sequence (GFP)-AEVs were constructed. NRCMs were isolated and counted, of which $1 \times 10^6$ cells were infected with miR-24-AEVs or GFP-AEVs for 24 h (MOI = 10), respectively. miR-24 was up-regulated in NRCMs by transferring the miR-24-AEVs compared with the negative control (miR-24 vs. GFP: 7.77 ± 2.50 vs. 0.96 ± 0.24, $t = -2.709$, $P < 0.05$) [Figure 2e]. The p27 mRNA expression exhibited a 44.85% reduction in NRMCs (miR-24 vs. GFP: 0.58 ± 0.05 vs. 1.06 ± 0.09, $t = 4.400$, $P < 0.01$) [Figure 2f] and p27 protein expression exhibited a 28.32% reduction in NRCMs (miR-24 vs. GFP: 0.71 ± 0.07 vs. 0.99 ± 0.05, $t = 3.503$, $P < 0.01$) [Figure 2g]. These results demonstrated that p27 was the target of miR-24.

## Overexpression of microRNA-24-induced cardiomyocyte hypertrophy

To determine the effects of up-regulated miR-24 overexpression on NRCMs, we observed the changes of NRCMs after transfection with miR-24-AEVs [Figure 2e].

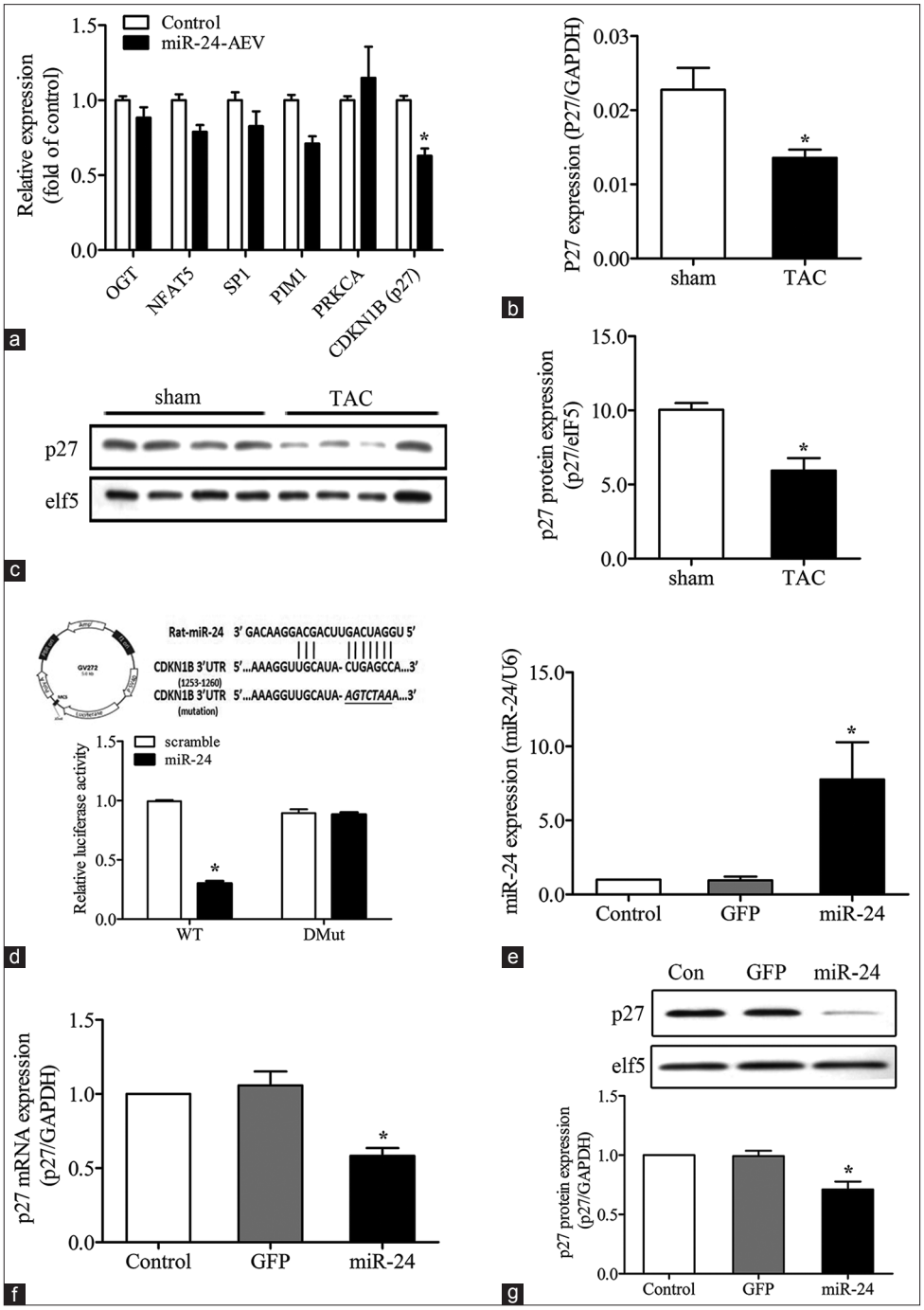


**Figure 2:** p27 was repressed by miR-24 in hypertrophic cardiac tissues and NRCMs. (a) qPCR analysis of potential target genes of miR-24. *$P < 0.05$ versus control. (b) p27 mRNA decreased in TAC rats. *$P < 0.05$ versus sham. (c) p27 protein decreased in TAC rats. *$P < 0.05$ versus sham. (d) Quantitative analysis of relative luciferase activity. *$P < 0.05$ versus scramble. (e) miR-24 expression was detected by qRT-PCR after transfection with miR-24-AEVs. *$P < 0.05$ versus GFP-AEVs. p27 mRNA (f) and protein (g) decreased in miR-24 over-expression group. *$P < 0.05$ versus GFP-AEVs. Data are shown as mean ± SE, $n = 6$. miR-24: MicroRNA-24; NRCMs: Neonatal rat cardiac myocytes; qPCR: Quantitative polymerase chain reaction; qRT-PCR: Quantitative real-time polymerase chain reaction; TAC: Transverse aortic constriction; AEVs: Adenoviral expression vector; GFP: Green Fluorescent Protein; SE: Standard error.

After 24-h transfection, the up-regulated miR-24-induced cardiomyocyte hypertrophy changes, including cell size enlargement and fetal gene reactivation. As shown in Figure 3, the expression of fetal genes, ANP, and BNP, were upregulated 2.58- and 4.52-fold, respectively (ANP: miR-24 vs. GFP, 2.13 ± 0.40 vs. 0.73 ± 0.07, $t = -3.415$, $P < 0.05$; BNP: miR-24 vs. GFP, 5.52 ± 0.98 vs. 1.22 ± 0.26, $t = -4.228$, $P < 0.01$) [Figure 3a and 3b]. Total protein expression was increased 1.16-fold (miR-24 vs. GFP: 1.22 ± 0.04 vs. 1.05 ± 0.02, $t = -3.621$, $P < 0.05$) [Figure 3c] and the mean cardiomyocyte size showed a 21.76% increase (miR-24 vs. GFP: 17.01 ± 0.76 vs. 13.97 ± 0.41,

**Table 1: The potential targets of miR-24**

| Targets | Full name (in human gene) | Possible functions in CV system | Rank (human) | Aggregate $P_{CT}$ (rat) | Rank (rat) |
|---|---|---|---|---|---|
| *OGT* | O-linked N-acetylglucosamine (GlcNAc) transferase (UDP-N-acetylglucosamine: polypeptide-N-acetylglucosaminyltransferase) | Mitochondrial calcium circulation | 284 | 0.48 | 209 |
| *NFAT5* | Nuclear factor of activated T-cells 5, tonicity-responsive | Cytotoxic survival | 372 | 0.59 | 301 |
| *SP1* | Sp1 transcription factor | Proliferation, hypertrophy | 321 | 0.60 | 177 |
| *PIM1* | Pim-1 oncogene | Anti-apoptosis, hypertrophy | 329 | 0.28 | 218 |
| *PRKCA* | Protein kinase C, alpha | Calcium ions, contractions of the coronary arteries | 392 | 0.28 | 319 |
| *CDKN1B* | Cyclin-dependent kinase inhibitor 1B (p27, Kip1) | Cell cycle, cardiac hypertrophy | 27 | 0.62 | 14 |

CV: Cardiovascular; miR-24: MicroRNA-24; $P_{CT}$: The probability of conserved targeting.

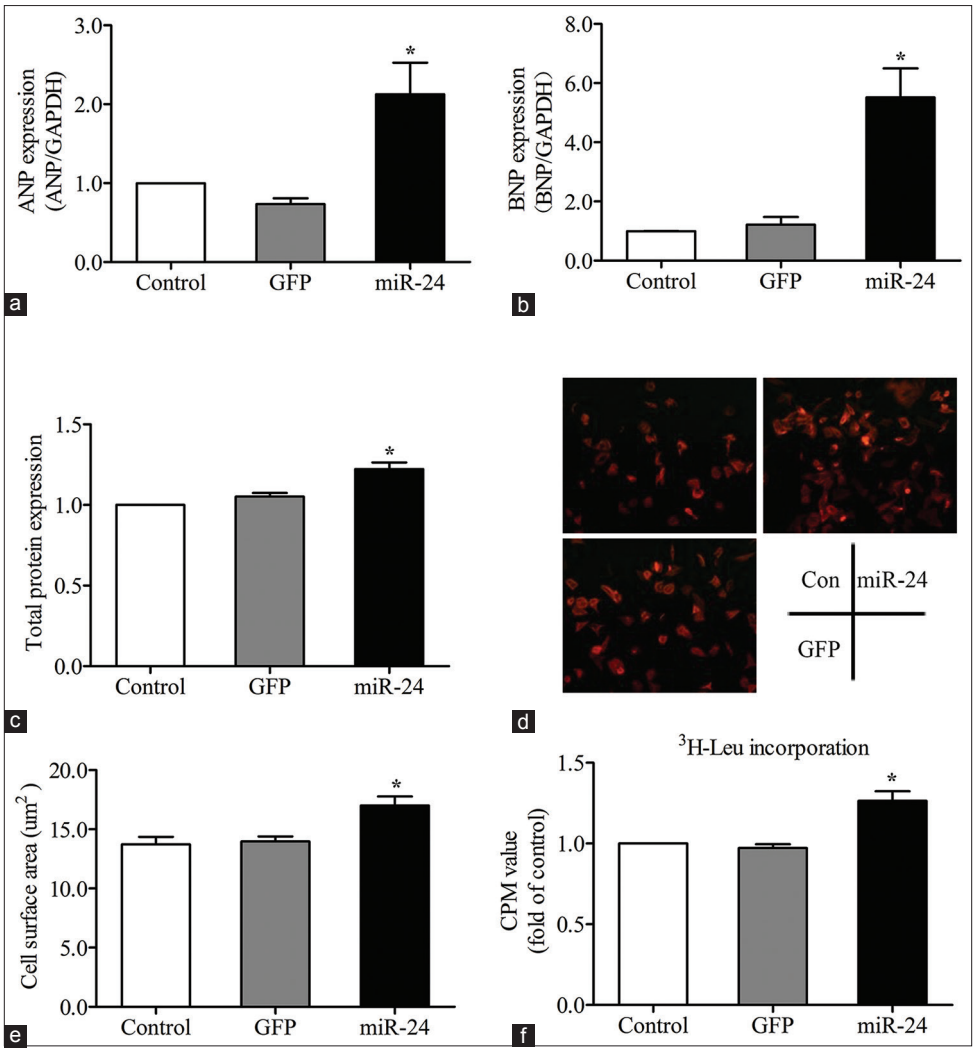


**Figure 3:** Overexpression of miR-24 led to NRCMs hypertrophy. (a) ANP increased in NRCMs after transfection with miR-24-AEVs. *$P < 0.05$ versus GFP-AEVs. (b) BNP increased after transfection with miR-24-AEVs. *$P < 0.05$ versus GFP-AEVs. (c) Total protein expression increased. *$P < 0.05$, compared with group GFP-AEVs. (d) The morphology of NRCMs was stained by F-actin (Original magnification ×100). (e) The statistical graph of cell surface of (d). *$P < 0.05$ versus GFP-AEVs. (f) Detection of total protein synthesis by $^3$H leucine intake method. *$P < 0.05$ versus GFP-AEVs. Data are shown as mean ± SE, $n = 5$. miR-24: MicroRNA-24; NRCMs: Neonatal rat cardiac myocytes; ANP: Atrial natriuretic factor; AEVs: Adenoviral expression vector; GFP: Green Fluorescent Protein; BNP: Brain natriuretic peptide; SE: Standard error.

$t = -3.497$, $P < 0.05$) [Figure 3d and 3e]. The detection of $^3$H-Leu incorporation showed that up-regulated miR-24 led to a 1.3-fold increase of total protein synthesis in cardiomyocytes (miR-24 vs. GFP: 1.26 ± 0.06 vs. 0.97 ± 0.02, $t = -4.603$, $P < 0.01$) [Figure 3f]. These results indicated that up-regulated miR-24 in cardiomyocytes led to the lower expression of p27 accompanied with cardiomyocyte hypertrophy.

### Overexpression of microRNA-24 led to the altered cell cycle in neonatal rat cardiac myocytes

As a target gene of miR-24, p27 is known as a cyclin-dependent kinase inhibitor, which is involved in regulating the cell cycle through inducing G0/G1 arrest. In the adenovirus-mediated overexpression, up-regulated miR-24 led to the lower expression of p27. To determine whether the up-regulated expression of miR-24 caused any changes in the cell cycle, flow cytometry was used to detect alterations in the cell cycle [Figure 4a-c]. It was shown that the G0/G1 phase population decreased from 87.97% to 81.21% (miR-24 vs. GFP: $t = -4.515$, $P < 0.01$) [Figure 4d], whereas the S phase population increased from 12.35% to 6.29% (miR-24 vs. GFP: $t = -3.453$, $P < 0.01$) [Figure 4e]. The percentage of G2/M phase cells was not significantly altered (miR-24 vs. GFP, $t = -0.334$, $P = 0.745$) [Figure 4f]. These results indicated that up-regulated miR-24 resulted in cardiac hypertrophy by affecting the G0/G1 arrest through down-regulation of p27 expression.

## Discussion

In the present study, we found that miR-24 expression increased in hypertrophic cardiac tissue and the up-regulated miR-24 would lead to cardiomyocyte hypertrophy. As a target gene of miR-24, p27 expression was decreased both in hypertrophic cardiac tissue and in NRCMs with miR-24 upregulation. The up-regulated miR-24 resulted in increased cell surface, total protein expression and cell cycle changes

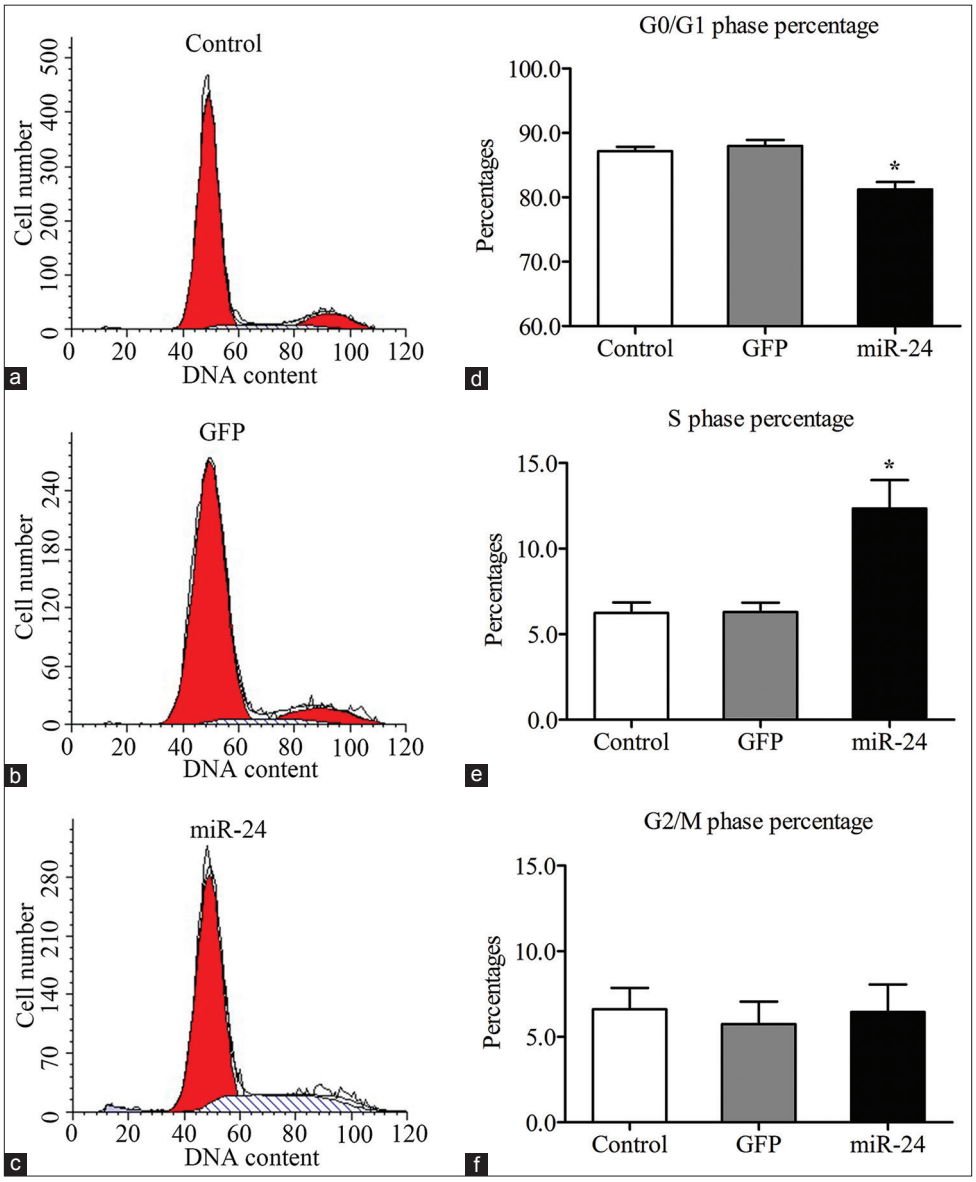


**Figure 4:** Effects of overexpression of miR-24 on cell cycle in NRCMs. (a-c) The first peaks are diploid cells, mainly G0 and G1 phase cells, the second peaks are tetraploid cells, mainly G2 and M phase cells, and the peaks between second peaks are distributed between cells that are undergoing DNA replication, which are phase S cells. (d) NRCMs in G0/G1 phase was decreased. *$P < 0.05$ versus GFP-AEVs. (e) NRCMs in S phase was increased. *$P < 0.05$ versus GFP-AEVs. (f) NRCMs transfected with miR-24-AEVs in G2/M phase was not significantly from group GFP-AEVs, $P > 0.05$. Data are shown as mean ± SE, $n = 5$. miR-24: MicroRNA-24; NRCMs: Neonatal rat cardiac myocytes; AEVs: Adenoviral expression vector; GFP: Green Fluorescent Protein; SE: Standard error.

in NRCMs. Our results suggested that miR-24 was a key mediator promoting cardiac hypertrophy, and one of the potential mechanisms was promoting cells in G0/G1 phase into S phase by repressing p27 expression.

miR-24 is extensively expressed in various tissues,[19] and it plays an important role in various physiological or pathological conditions, such as heart failure, oral cancers, prostate cancer, hyperglycemia, and Alzheimer's disease.[20-24] In the present study, miR-24 was found to participate in the process of cardiac hypertrophy in rats, and the up-regulated expression of miR-24 in NRCMs led to the higher expression of ANP and BNP, the higher expression of the total protein, the higher increase of cell surface area and CPM in $^{3}$H-Leu incorporation. These results showed that abnormally increased miR-24 promoted cardiac hypertrophy, which is not a concomitant phenomenon of cardiac hypertrophy. In general, cardiac myocytes rapidly proliferate during fetal life but withdraw from the cell cycle and lose the ability of proliferation soon after birth in mammals.[25,26] Although to what extent adult cardiac myocytes proliferate is controversial, it appears that the cell cycle changes are involved in cardiac hypertrophy in a predominant form of an increase in cell size (hypertrophy), but not in number.[27]

As a kind of cyclin-dependent kinase (CDK) inhibitors (CKIs), p27 extensively suppresses the activities of various cyclins and CDKs, which drive forward the cell cycle, and consequently, cells in G0/G1 phase cannot enter into the S phase of cell cycle.[28] This is important in inhibiting the proliferation of tumor cells.[29,30] However, p27-knockout mice were reported to develop age-dependent cardiac hypertrophy and had exaggerated hypertrophic responses to aortic banding.[31] Recent evidence suggested that miRNAs controlled the levels of multiple cell cycle regulators, thus controlling cell proliferation, and miR-24 was reported to promote cell proliferation by targeting p27 in primary keratinocyte and different cancer types.[22,32] In our study, miR-24 up-regulation in NRCMs induced the down-regulation of p27, leading to cardiomyocyte hypertrophy. Analysis of the cell cycle showed that the percentage of cells in G0/G1 phase decreased, the percentage of cells in S phase increased, and the percentage of cells in G2/M phase remained unchanged. This suggested that the cell cycle changes in NRCMs resulted in cardiomyocyte hypertrophy. As the luciferase report assay showed that p27 was targeted by miR-24, we suggested that miR-24 could induce cardiac hypertrophy through repressing p27 expression.

In conclusion, the present study showed that miR-24 was a key mediator of cardiac hypertrophy by repressing p27 expression, which led to S phase arrest. As many other miRNAs and CKIs are involved in cell cycle changes,[33] more in-depth studies are needed.

*Supplementary information is linked to the online version of the paper on the Chinese Medical Journal website.*


## Financial support and sponsorship

This work was supported by grant from National Natural Science Foundation of China (No. 91339105, and No. 81625001).


## Conflicts of interest

There are no conflicts of interest.

## References


1. Yano K, Grove JS, Reed DM, Chun HM. Determinants of the prognosis after a first myocardial infarction in a migrant Japanese population. The Honolulu Heart Program. Circulation 1993;88:2582-95. doi: 10.1161/01.CIR.88.6.2582.
2. Wang S, Xue H, Zou Y, Sun K, Fu C, Wang H, *et al.* Left ventricular hypertrophy, abnormal ventricular geometry and relative wall thickness are associated with increased risk of stroke in hypertensive patients among the Han Chinese. Hypertens Res 2014;37:870-4. doi: 10.1038/hr.2014.88.
3. Yuan Y, Zhang Y, Han X, Li Y, Zhao X, Sheng L, *et al.* Relaxin alleviates TGFβ1-induced cardiac fibrosis via inhibition of Stat3-dependent autophagy. Biochem Biophys Res Commun 2017;493:1601-7. doi: 10.1016/j.bbrc.2017.09.110.
4. Zhao CH, Ma X, Guo HY, Li P, Liu HY. RIP2 deficiency attenuates cardiac hypertrophy, inflammation and fibrosis in pressure overload induced mice. Biochem Biophys Res Commun 2017;493:1151-8. doi: 10.1016/j.bbrc.2017.07.035.
5. Bénard L, Oh JG, Cacheux M, Lee A, Nonnenmacher M, Matasic DS, *et al.* Cardiac stim1 silencing impairs adaptive hypertrophy and promotes heart failure through inactivation of mTORC2/Akt signaling. Circulation 2016;133:1458-71. doi: 10.1161/CIRCULATIONAHA.115.020678.
6. Lee RC, Ambros V. An extensive class of small RNAs in Caenorhabditis elegans. Science 2001;294:862-4. doi: 10.1126/science.1065329.
7. Heggermont WA, Papageorgiou AP, Quaegebeur A, Deckx S, Carai P, Verhesen W, *et al.* Inhibition of microRNA-146a and overexpression of its target dihydrolipoyl succinyltransferase protect against pressure overload-induced cardiac hypertrophy and dysfunction. Circulation 2017;136:747-61. doi: 10.1161/CIRCULATIONAHA.116.024171.
8. Wang D, Zhai G, Ji Y, Jing H. MicroRNA-10a targets T-box 5 to inhibit the development of cardiac hypertrophy. Int Heart J 2017;58:100-6. doi: 10.1536/ihj.16-020.
9. Guan X, Wang L, Liu Z, Guo X, Jiang Y, Lu Y, *et al.* MiR-106a promotes cardiac hypertrophy by targeting mitofusin 2. J Mol Cell Cardiol 2016;99:207-17. doi: 10.1016/j.yjmcc.2016.08.016.
10. Wang J, Liew OW, Richards AM, Chen YT. Overview of microRNAs in cardiac hypertrophy, fibrosis, and apoptosis. Int J Mol Sci 2016;17. pii: E749. doi: 10.3390/ijms17050749.
11. van Rooij E, Sutherland LB, Liu N, Williams AH, McAnally J, Gerard RD, *et al.* A signature pattern of stress-responsive microRNAs that can evoke cardiac hypertrophy and heart failure. Proc Natl Acad Sci U S A 2006;103:18255-60. doi: 10.1073/pnas.0608791103.
12. Haeusler AR, Donnelly CJ, Periz G, Simko EA, Shaw PG, Kim MS, *et al.* C9orf72 nucleotide repeat structures initiate molecular cascades of disease. Nature 2014;507:195-200. doi: 10.1038/nature13124.
13. Lu M, Shi B, Wang J, Cao Q, Cui Q. TAM: A method for enrichment and depletion analysis of a microRNA category in a list of microRNAs. BMC Bioinformatics 2010;11:419. doi: 10.1186/1471-2105-11-419.
14. MacLellan WR, Schneider MD. Genetic dissection of cardiac growth control pathways. Annu Rev Physiol 2000;62:289-319. doi: 10.1146/annurev.physiol.62.1.289.
15. Xu M, Wu HD, Li RC, Zhang HB, Wang M, Tao J, *et al.* Mir-24 regulates junctophilin-2 expression in cardiomyocytes. Circ Res 2012;111:837-41. doi: 10.1161/CIRCRESAHA.112.277418.
16. Iwatsubo K, Minamisawa S, Tsunematsu T, Nakagome M, Toya Y, Tomlinson JE, *et al.* Direct inhibition of type 5 adenylyl cyclase prevents myocardial apoptosis without functional deterioration. J Biol Chem 2004;279:40938-45. doi: 10.1074/jbc.M314238200.
17. Kiraz HA, Poyraz F, Kip G, Erdem Ö, Alkan M, Arslan M, *et al.* The effect of levosimendan on myocardial ischemia-reperfusion injury in

streptozotocin-induced diabetic rats. Libyan J Med 2015;10:29269. doi: 10.3402/ljm.v10.29269.
18. Rockman HA, Ross RS, Harris AN, Knowlton KU, Steinhelper ME, Field LJ, *et al.* Segregation of atrial-specific and inducible expression of an atrial natriuretic factor transgene in an *in vivo* murine model of cardiac hypertrophy. Proc Natl Acad Sci U S A 1991;88:8277-81. doi: 10.1073/pnas. 88.18.8277.
19. Landgraf P, Rusu M, Sheridan R, Sewer A, Iovino N, Aravin A, *et al.* A mammalian microRNA expression atlas based on small RNA library sequencing. Cell 2007;129:1401-14. doi: 10.1016/j.cell. 2007.04.040.
20. Li RC, Tao J, Guo YB, Wu HD, Liu RF, Bai Y, *et al. In vivo* suppression of microRNA-24 prevents the transition toward decompensated hypertrophy in aortic-constricted mice. Circ Res 2013;112:601-5. doi: 10.1161/CIRCRESAHA.112.300806.
21. Liu X, Wang A, Heidbreder CE, Jiang L, Yu J, Kolokythas A, *et al.* MicroRNA-24 targeting RNA-binding protein DND1 in tongue squamous cell carcinoma. FEBS Lett 2010;584:4115-20. doi: 10.1161/CIRCRESAHA.112.300806.
22. Lynch SM, McKenna MM, Walsh CP, McKenna DJ. MiR-24 regulates CDKN1B/p27 expression in prostate cancer. Prostate 2016;76:637-48. doi: 10.1002/pros.23156.
23. Xiang Y, Cheng J, Wang D, Hu X, Xie Y, Stitham J, *et al.* Hyperglycemia repression of miR-24 coordinately upregulates endothelial cell expression and secretion of von Willebrand factor. Blood 2015;125:3377-87. doi: 10.1182/blood-2015-01-620278.
24. Müller M, Kuiperij HB, Claassen JA, Küsters B, Verbeek MM. MicroRNAs in Alzheimer's disease: Differential expression in hippocampus and cell-free cerebrospinal fluid. Neurobiol Aging 2014;35:152-8. doi: 10.1016/j.neurobiolaging.2013.07.005.
25. Li F, Wang X, Capasso JM, Gerdes AM. Rapid transition of cardiac myocytes from hyperplasia to hypertrophy during postnatal development. J Mol Cell Cardiol 1996;28:1737-46. doi: 10.1006/jmcc.1996.0163.
26. Bicknell KA, Coxon CH, Brooks G. Can the cardiomyocyte cell cycle be reprogrammed? J Mol Cell Cardiol 2007;42:706-21. doi: 10.1016/j.yjmcc.2007.01.006.
27. Ahuja P, Sdek P, MacLellan WR. Cardiac myocyte cell cycle control in development, disease, and regeneration. Physiol Rev 2007;87:521-44. doi: 10.1152/physrev.00032.2006.
28. Chu IM, Hengst L, Slingerland JM. The Cdk inhibitor p27 in human cancer: Prognostic potential and relevance to anticancer therapy. Nat Rev Cancer 2008;8:253-67. doi: 10.1038/nrc2347.
29. Wang Z, Smith KS, Murphy M, Piloto O, Somervaille TC, Cleary ML, *et al.* Glycogen synthase kinase 3 in MLL leukaemia maintenance and targeted therapy. Nature 2008;455:1205-9. doi: 10.1038/nature07284.
30. Newbold A, Salmon JM, Martin BP, Stanley K, Johnstone RW. The role of p21(waf1/cip1) and p27(Kip1) in HDACi-mediated tumor cell death and cell cycle arrest in the Eμ-myc model of B-cell lymphoma. Oncogene 2014;33:5415-23. doi: 10.1038/onc.2013.482.
31. Li J, Zhang C, Xing Y, Janicki JS, Yamamoto M, Wang XL, *et al.* Up-regulation of p27(kip1) contributes to Nrf2-mediated protection against angiotensin II-induced cardiac hypertrophy. Cardiovasc Res 2011;90:315-24. doi: 10.1093/cvr/cvr010.
32. Xiao S, Wang X, Ni H, Li N, Zhang A, Liu H, *et al.* MicroRNA miR-24-3p promotes porcine reproductive and respiratory syndrome virus replication through suppression of heme oxygenase-1 expression. J Virol 2015;89:4494-503. doi: 10.1128/JVI.02810-14.
33. Lim S, Kaldis P. Cdks, cyclins and CKIs: Roles beyond cell cycle regulation. Development 2013;140:3079-93. doi: 10.1242/dev. 091744.

# microRNA-24促进大鼠心肌肥厚的发生


## 摘要

**背景**：MicroRNA-24通过下调心肌兴奋-收缩耦联效率从而在心力衰竭中发挥重要的调控作用。长期的心肌肥厚导致心力衰竭的发生，然而，miR-24在心肌肥厚中的作用尚未被广泛了解。本研究初步探究了miR-24在心肌肥厚中的作用及其作用机制。

**方法**：12只体重为50 ± 5 g 的SD大鼠随机分为两组，主动脉弓缩窄组（TAC）与对照组（sham）。超声心动图和苏木精-伊红染色用于评估心肌肥厚指标。通过TargetScans软件计算预测miR-24的靶基因，同时利用实时荧光定量PCR与荧光素酶报告基因实验进行验证。在乳大鼠心肌细胞中过表达miR-24后，使用免疫荧光实验测量细胞表面积的变化，利用$^{3}$H亮氨酸掺入法检测心肌细胞总蛋白合成，以及采用流式细胞术分析观察细胞周期的变化。

**结果**：miR-24在主动脉宫缩窄的大鼠心肌组织中的表达异常升高（$t$=-2.938，$P$<0.05）。TargetScans分析结果显示细胞周期调节因子CDKN1B （p27, Kip1）是miR-24的潜在靶基因，同时荧光素酶报告基因实验证实了miR-24与p27的靶效关系。同时，我们的结果显示p27在主动脉宫缩窄的大鼠心肌组织中的表达显著降低（$t$=2.896，$P$<0.05）。此外，在乳大鼠心肌细胞中过表达miR-24会导致p27表达水平的下降（$t$=4.400，$P$<0.01），造成细胞周期G0/G1期阻滞的降低，以及心肌细胞肥大表型的变化。

**结论**：miR-24通过下调p27的表达影响细胞周期进程，从而促进心肌肥厚的发生。

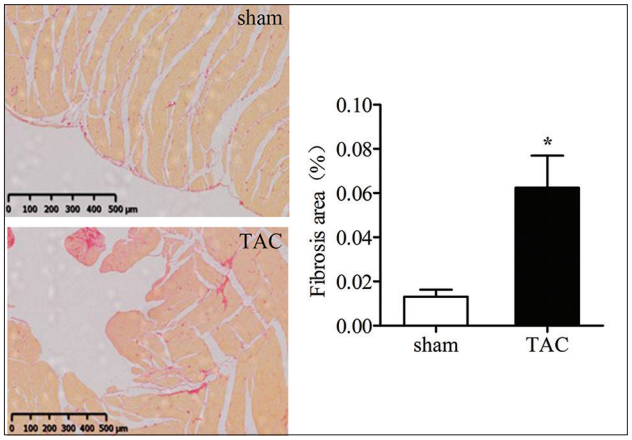


**Supplementary Figure 1:** Sirius Red stain of cardiac tissue in TAC rats. The collagen of the heart was stained by Sirius Red to observe the effect of the TAC surgery. *$P < 0.05$ versus sham. Data are shown as mean ± SE, $n = 6$. TAC: Transverse aortic constriction; SE: Standard error.

**Supplementary Table 1: Statistical results for the TAC mouse models**

| Clinical characteristics | Sham | TAC |
|---|---|---|
| LVAW;d (mm) | 1.12 ± 0.15 | 2.60 ± 0.15* |
| LVAW;s (mm) | 3.03 ± 0.13 | 3.90 ± 0.19* |
| LVID;d (mm) | 8.07 ± 0.34 | 7.77 ± 0.23 |
| LVID;s (mm) | 23.10 ± 1.00 | 32.00 ± 1.50 |
| LVPW;d (mm) | 1.99 ± 0.10 | 2.99 ± 0.10* |
| LVPW;s (mm) | 3.11 ± 0.15 | 3.81 ± 0.16* |
| EF (%) | 69.23 ± 2.00 | 73.12 ± 3.20 |
| FS (%) | 40.50 ± 1.62 | 44.06 ± 2.83 |
| LV mass AW (mg) | 969.10 ± 34.20 | 1469.00 ± 140.60* |
| LV VOL;d (ul) | 355.10 ± 31.24 | 324.2 ± 21.55 |
| LV VOL;s (ul) | 110.80 ± 13.91 | 86.71 ± 11.64 |
| Weight (g) | 629.00 ± 30.62 | 562.80 ± 13.38 |
| Heart weight (mg) | 1509.00 ± 88.48 | 1848.00 ± 27.59* |
| Heart weight/weight (mg/g) | 2.35 ± 0.11 | 3.30 ± 0.12* |
| Tibia length (mm) | 48.15 ± 1.12 | 44.75 ± 0.52* |
| Heart weight/tibia length (mg/mm) | 31.42 ± 2.02 | 41.34 ± 1.02* |

*$P$<0.05 versus sham, $n = 6$. LVAW;d: Left ventricular anterior diastolic wall thickness; LVAW;s: Left ventricular anterior systolic wall thickness; LVID;d: Left ventricular end diastolic diameter; LVID;s: Left ventricular end systolic diameter; LVPW;d: Left ventricular posterior diastolic wall thickness; LVPW;s: Left ventricular posterior systolic wall thickness; EF: Ejection fraction; FS: Fractional shortening; LV mass AW: Left ventricular mass AW; LV VOL;d: Left ventricular end diastolic volume; LV VOL;s: Left ventricular end systolic volume; TAC: Transverse aortic constricted.

| | |
|---|---|
| miR-24 | 3'-GACAAGGACGACUUGACUCGGU-5' |
| Chimp | 5'-AAA- AGGUUGCAUACUGAGCCAAG------UAUA |
| Human | 5'-AAA- AGGUUGCAUACUGAGCCAAG------UAUA |
| Rhesus | 5'-AAA- AGGUUGCAUACUGAGCCAAG------UAUA |
| Squirrel | 5'-- AA- AGGUUGCAUACUGAGCCAAG------UAUA |
| Mouse | 5'-AAA- AGGUUGCAUACUGAGCCAAG------UAUA |
| Rat | 5'-AAA- AGGUUGCAUACUGAGCCAAG------UAUA |
| Rabbit | 5'-AAA- AGGUUGCAUACUGAGCCAAG------UAUA |
| Pig | 5'-AAA- AGGUUGCAUACUGAGCCAAG------UAUA |
| Cow | 5'-AAA- AGGUUGCAUACUGAGCCAAG------UAUA |
| Cat | 5'-AAA- AGGUUGCAUACUGAGCCAAG------UAUA |
| Dog | 5'-AAA- AGGUUGCAUACUGAGCCAAG------UAUA |
| Brown bat | 5'-AAA- AGGUUGCAUACUGAGCCAAG------UAUA |
| Elephant | 5'-AAA- AGGUUGCAUACUGAGCCAAG------UAUA |
| Opossum | 5'-AAA- AGGUUGCAUACUGAGCCAAG------UAUA |

**Supplementary Figure 2:** The potential miR-24 target sites in the 3'UTR of p27. The potential target sites in the 3'UTR of p27 were conserved in different species. The sequences were aligned using TargetScan http://www.targetscan.org/vert_71/. 3'UTR: Untranslated region; miR-24: MicroRNA-24.